R&D FOR A SUPER COMPACT SLED SYSTEM AT SLAC*

Juwen W. Wang†, Sami G. Tantawi, Chen Xu, Matt Franzi, Patrick Krejcik, Gordon Bowden, Shantha Condamoor, Yuantao Ding, Valery Dolgashev, John Eichner, Andrew Haase, James R. Lewandowski, Liling Xiao, SLAC National Accelerator Laboratory, Menlo Park, CA 94025, USA

Abstract

We have successfully designed, fabricated, installed and tested a super compact X-Band SLED system at SLAC. It is composed of an elegant 3dB coupler / mode converter / polarizer and a single spherical energy storage cavity with high Q_0 of 94000 and diameter less than 12 cm. The available RF peak power of 50 MW can be compressed to a peak average power of more than 200 MW in order to double the kick for the electron bunches in a RF transverse deflector system and greatly improve the measurement resolution of both the electron bunches and the X-ray FEL pulses. High power operation has demonstrated the excellent performance of this RF compression system without RF breakdown, sign of pulse heating and RF radiation. The design physics and fabrication as well as the measurement results will be presented in detail.

INTRODUCTION

This diagnostics for X-ray temporal measurement based on the transverse deflectors, the magnetic spectrometer and the Ce:YAG screen located downstream of the FEL undulator has been intensively used at the LCLS operation [1]. Its layout is shown in Figure 1.

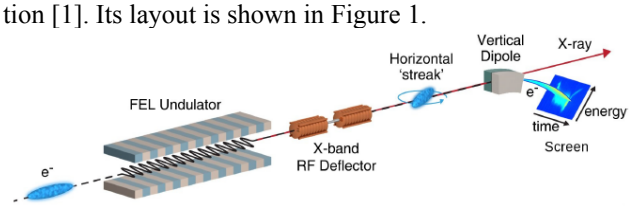

Figure 1: Diagnostics layout of the X-ray temporal measurement at the LCLS.

In order to improve temporal resolution, we have designed and fabricated a novel super compact SLED system to double the peak deflection. [2] This paper describes its principle, design and technical advances.

DESIGN OF SUPER COMPACT SLED SYSTEM

More than forty years ago, SLAC developed the SLED system to obtain high peak RF power in exchange for the RF pulse length reduction [3]. The key components of a SLED system include a 3dB coupler with two 90° apart power ports and two high Q energy storage cavities.

The LCLS deflector is made of two traveling structures, Each one is a 1.0 m long, constant impedance structure with transverse impedance of 41.9 MΩ/m, filling time T_f=106 ns (group velocity of -3.165 % speed of light) and attenuation factor τ=0.62 Neper. If we assume the similar average RF power of 106 ns pulses for both the SLEDed pulse and non SLEDed flat pulses to feed a backward wave constant impedance deflector, the corresponding kick voltages are shown in Fig. 2.

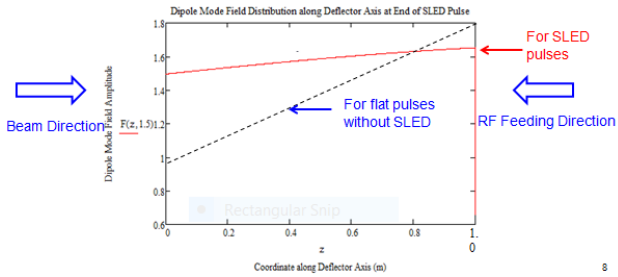

Figure 2: Kick voltage along the deflector structure.

We need to optimize the SLED system by calculating its total gain for various coupling coefficients for the high Q_0 cavity, its Q values and pulse length. Figure 3 shows that the highest gain of larger than factor of 2 can be obtained for Q_0 ~$9x10^4$ and 1μs pulses if the over-coupling coefficient β is optimized to be 7-8 for 11424 MHz.

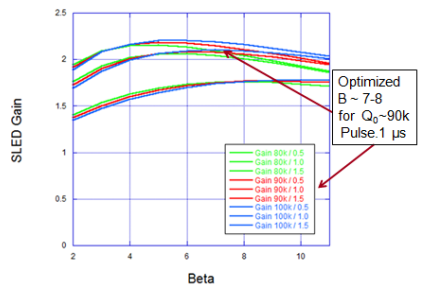

Figure 3: SLED gain as function of pulse widths and Q_0 values of energy storage cavity.

Unified 3dB Coupler / Mode convertor / Polarizer

Having all the basic functions of a 3dB coupler, a much more compact and elegant dual-mode circular polarizer was developed to transform the TE_{01} mode in a rectangular waveguide into two polarized TE_{11} modes in quadrature in a circular waveguide as shown in Fig. 4.

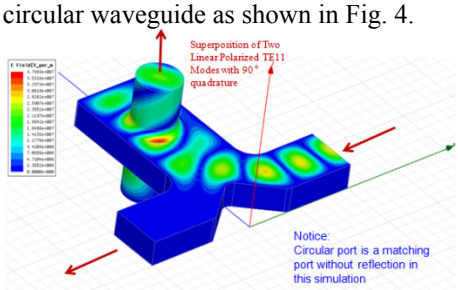

Figure 4: Schematic view of the dual-mode polarizer.

The input TE_{01} mode converts to both TE_{01} and TE_{02} modes in a widened rectangular waveguide region, and their magnetic field components will couple to two per-

* Work supported by DOE contract DE-AC03-76SF00515.
† Email address jywap@slac.stanford.edu

ISBN 978-3-95450-147-2

pendicular polarized TE_{11} modes in the circular waveguide. We adjusted geometries so the phases of the two polarized modes are in quadrature.

If the circular waveguide feeds a spherical cavity as shown in Fig. 5, two corresponding polarized sphere modes will act in similar fashion to the two modes from the two cylinders in a traditional SLED system.

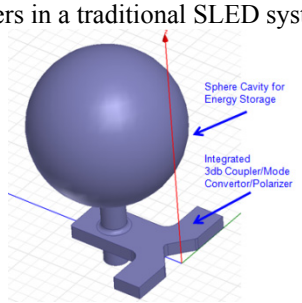

Figure 5: Construction of the new SLED system.

High Q Sphere Cavity

The electrical vector potential F for all modes in a sphere with radius r=a can be described as:

$$(F_r)_{mnp} = \hat{J}_n\left(u_{np}\frac{r}{a}\right)P_n^m(\cos\vartheta)\begin{Bmatrix}\cos m\varphi\\ \sin m\varphi\end{Bmatrix},$$

where $\hat{J}_n$ is the spherical Bessel Function and P_n^m are the associated Legendre Polynomials with $m \leq n$.

For TE modes, $E_\varphi = H_\theta = 0$ at surface r=a. This means $\hat{J}_n(u_{np})=0$. Therefore, the sphere radius can be calculated using wave propagation constant k and value of u_{np}.

$$a = \frac{u_{np}}{k} = \frac{c \times u_{np}}{k} = 0.41767u_{np}\ (cm)$$

Sphere radius is independent with mode index m, there are numerous degenerative modes with the same m.

In our case, we have chosen TE_{m14} modes. There are three possible modes:

$$(F_r)_{014} = \hat{J}_1\left(14.066\frac{r}{a}\right)\cos\vartheta$$

$$(F_r)_{114} = \hat{J}_1\left(14.066\frac{r}{a}\right)\sin\vartheta\cos\varphi$$

$$(F_r)_{114} = \hat{J}_1\left(14.066\frac{r}{a}\right)\sin\varphi$$

For a perfect spherical cavity, these three modes have the same mode patterns except that they are rotated 90° in space from each other, which can be seen in following Fig. 6 and Fig. 7.

In reality, they can be slightly distinguished in frequencies due to the perturbation from the coupler port. The TE_{014} mode is higher in frequency and very weakly undercoupled due to the feed orientation.

Another interesting property is the sole dependence of Q_0 on the sphere radius without depending on the mode types. The quality factor Q_0 for TE Modes is

$$Q_0 = \frac{a}{\delta}$$

δ is the skin depth, for copper it is 0.61μm at 11 GHz.

Figure 6 shows two polarized TE_{114} modes of 11424 MHz as working SLED modes with Q_0~$9.5\text{x}10^4$ and overcoupling of 7-8 and a TE_{014} mode with 7 MHz higher in frequency, which has very weakly undercoupled due to its field pattern.

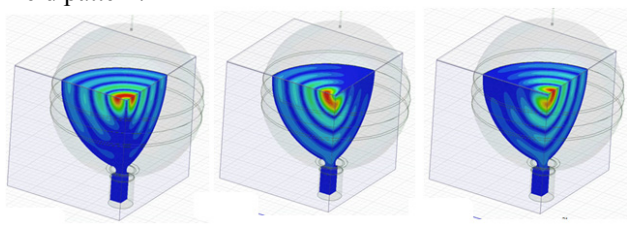

Figure 6: Two polarized TE_{114} modes (middle and right) and one TE_{014} mode (left).

Figure 7 schematically shows the wave propagation in the SLED system.

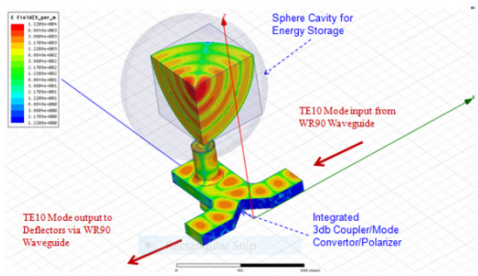

Figure 7: The wave propagation in the SLED system.

Coupler Design

The coupling iris between circular guide and sphere cavity was optimized to reduce the RF pulse heating. The final iris has rounding radius of 3 mm to make the pulse heating less than 40°C for 1.5 μs square pulses at peak power of 50 MW.

Mechanical Design and Assembly

Figure 8 and 9 show some pictures for the fabricated polarizer and SLED assembly.

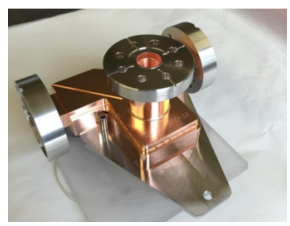

Figure 8: 3dB Coupler/ Mode Convertor / Polarizer.

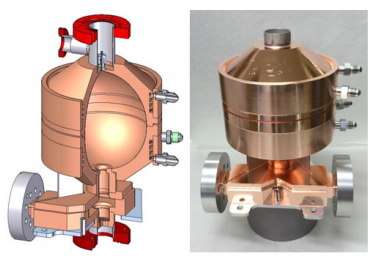

Figure 9: Mechanical design and fabricated SLED assembly.

A provide adequate pumping, a vacuum port was built on the bottom of the polarizer (see Fig. 9).

Tuning of the sphere cavity was well performed by combination of machining away a ridge in the sphere

equator during cold test and minor push-pull tuning on the top region of the finished sphere.

MICROWAVE MEASUREMENTS

Figures 10, 11 and 12 show the excellent performance of the polarizer by the microwave measurements.

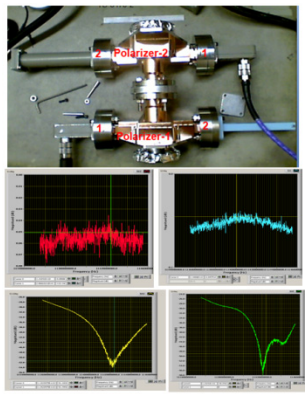

Figure 10: The transmission is -0.04 dB for two back-to-back polarizers with the transmission efficiency of 99%. The reflection from the input port is negligible -45db.

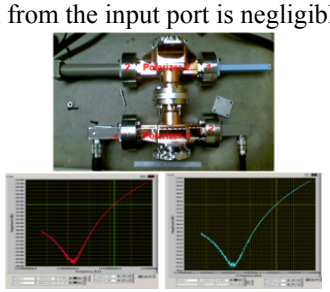

Figure 11: Isolation between in/out WR90 ports is -31 db.

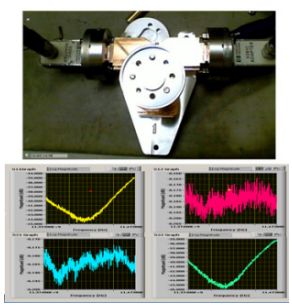

Figure 12: Proof of full SLEDed power transmission with the end of circular waveguide shorted.

The cold test for the fabricated SLED system has demonstrated great consistency of its microwave properties with the theoretical design as shown in Figs. 13 and 14.

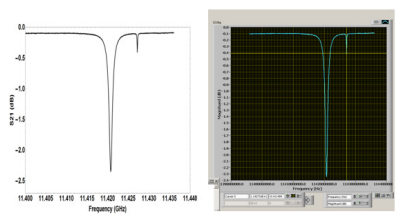

Figure 13: Frequency scan showing the two overlapped working modes TE_{114} (large) and a 7 MHz higher frequency mode TE_{014} (small) for theoretical design (left and measurement (right).

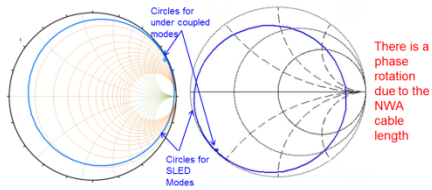

Figure 14: Smith Chart showing overcoupled working mode (large circle) and undercoupled mode (tiny circle) for theoretical design (left) and measurement (right).

HIGH POWER OPERATION

The SLED system was high power processed on an X-Band station at the SLAC Test Lab, then was installed at the LCLS between the klystron and upstream transmission line to the deflectors as shown in Fig. 15. The RF waveforms for the high power operation in comparison with the theoretical calculation is shown in Fig. 16.

Maximum kick has increased from 45 MV without SLED to 85 MV during recent operation. Full klystron power has not been reached the maximum. It was limited by a power line AC transformer, already updated, we are waiting for a machine maintenance time slot to push klystron power from present level to 50 MW. The maximum kick will reach the final goal of 95 MV (~10% more).

The system has been running encouragingly stable without breakdown, sign of pulse heating, outgassing or RF contact radiation near the SLED cavity body.

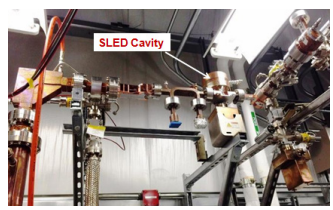

Figure 15: The SLED system has been installed.

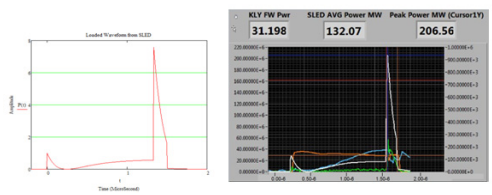

Figure 16: High power operation waveforms for theoretical design (left and measurement (right).

SUMMARY

This progress has proved great success for the X-Band super compact SLED system R&D.

The design can be easily extended to C- or S-Band. A broad range of future applications are on the horizon. Possibilities for flat top pulse compression system are under studies.

REFERENCES

[1] C. Behrens et al., Nature Communications, 5. 3762 2014.
[2] J, W. Wang et al. LINC2014, 2014.
[3] Z.D. Farkas et al., SLAC-PUB-1453, June, 1974.

ISBN 978-3-95450-147-2